AIP | Journal of Applied Physics

Epi-cleaning of Ge/GeSn heterostructures

L. Di Gaspare, D. Sabbagh, M. De Seta, A. Sodo, S. Wirths, D. Buca, P. Zaumseil, T. Schroeder, and G. Capellini

Citation: Journal of Applied Physics **117**, 045306 (2015); doi: 10.1063/1.4906616
View online: http://dx.doi.org/10.1063/1.4906616
View Table of Contents: http://scitation.aip.org/content/aip/journal/jap/117/4?ver=pdfcov
Published by the AIP Publishing

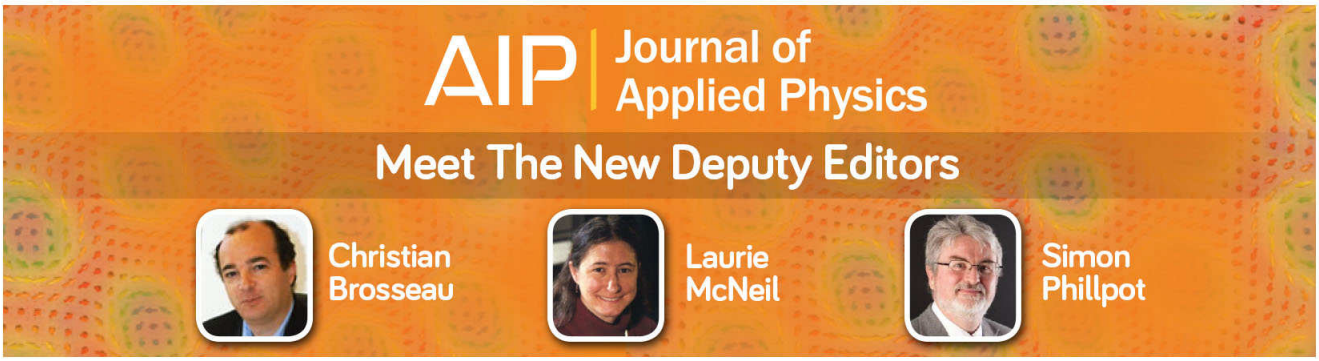

JOURNAL OF APPLIED PHYSICS **117**, 045306 (2015)

Epi-cleaning of Ge/GeSn heterostructures

L. Di Gaspare,[1] D. Sabbagh,[1] M. De Seta,[1] A. Sodo,[1] S. Wirths,[2] D. Buca,[2] P. Zaumseil,[3] T. Schroeder,[3,4] and G. Capellini[1,3,a)]
[1]*Dipartimento di Scienze, Università Roma Tre, Viale Marconi 446, 00146 Rome, Italy*
[2]*Peter Grünberg Institute 9 and JARA-Fundamentals of Future Information Technologies, Forschungszentrum Juelich, Juelich 52425, Germany*
[3]*IHP, Im Technologiepark 25, 15236 Frankfurt (Oder), Germany*
[4]*BTU Cottbus, Konrad-Zuse Str. 1, 03046 Cottbus, Germany*

(Received 13 October 2014; accepted 14 January 2015; published online 26 January 2015)

We demonstrate a very-low temperature cleaning technique based on atomic hydrogen irradiation for highly (1%) tensile strained Ge epilayers grown on metastable, partially strain relaxed GeSn buffer layers. Atomic hydrogen is obtained by catalytic cracking of hydrogen gas on a hot tungsten filament in an ultra-high vacuum chamber. X-ray photoemission spectroscopy, reflection high energy electron spectroscopy, atomic force microscopy, secondary ion mass spectroscopy, and micro-Raman showed that an O- and C-free Ge surface was achieved, while maintaining the same roughness and strain condition of the as-deposited sample and without any Sn segregation, at a process temperature in the 100–300 °C range. © *2015 AIP Publishing LLC*.
[http://dx.doi.org/10.1063/1.4906616]

INTRODUCTION

Semiconductor heterostructures based on the Ge/GeSn system have recently attracted wide interest owing to their peculiar band structure and to their possible use in innovative optoelectronic devices and in high performance microelectronic devices.[1] Multi quantum well structures and superlattices based on tensile strained Ge/GeSn virtual substrates have been proposed as active materials for infrared light emitting devices integrated in a silicon-based photonic platform.[2–4] In these systems, owing to the α-Sn vs Ge lattice mismatch (∼14%), the GeSn relaxed buffer layer induces in Ge a biaxial tensile strain parallel to the sample surface ε_{par}, which profoundly modifies its band structure, transforming it in a quasi-direct band gap semiconductor for $\varepsilon_{par} > 1.6\%$.[5] Progress in out-of equilibrium epitaxy has made available wafer-size Ge/GeSn virtual substrate deposited on Si(001) with Sn content in excess of 10%[6,7] but their use is still limited mainly because of the inherent difficulties of a cleaning procedure for the Ge epi-layer compatible with thermodynamical constrains of the GeSn system, which will be discussed in the following.

The cleaning of germanium surfaces for a subsequent epitaxial growth (epi-cleaning) is usually based on an *ex situ* chemical pre-clean completed by an *in situ* annealing step. The *ex situ* chemical treatment is used to remove the native oxide and metal contaminants and to grow a chemical Ge oxide layer protecting the epi-surface from contamination, which is subsequently desorbed in the vacuum chamber where the epitaxial growth will then be performed.[8] In order to remove the Ge sub-oxide (GeO_x, $x \leq 2$), the *ex situ* treatment contains also solutions including an oxidizing agent, such as H_2O_2, that oxidizes GeO_x into soluble GeO_2. The Ge substrate, now protected by its "clean" oxide, is then *in situ* annealed at relatively high temperature, at least 600 °C (Ref. 9) and with typical values ranging in the 700–800 °C range, to obtain an oxide- and contamination-free surface ready for the subsequent epitaxial deposition process.[10] Alternative standard cleaning routes comprises an intermediate, *in vacuo* ion-sputtering step with the aim of roughly removing the contaminated region close to the Ge free surface[11] or the use of *in situ* oxygen plasma to remove contaminants and grow a new high purity oxide layer, which is then desorbed by a thermal annealing.[12] Some authors suggest to complete the epi-cleaning procedure with a surface regrowth step having the purpose to "cure" the surface after the harsh sputtering and/or thermal annealing processes.[9,10] All the discussed *in situ* process steps involve temperatures at which Ge/GeSn structures are unstable.[1] In fact, the semiconducting diamond lattice α-GeSn phase, needed for the epitaxial growth of GeSn alloy, is stable only at temperatures below 13.2 °C. Moreover, Sn has low eutectic temperature of approximately 230 °C for alloying in Ge and its thermal equilibrium solid solubility is ∼1% only. As a consequence, the precipitation of metallic Sn clusters and Sn segregation on the GeSn surface is observed at temperatures exceeding the growth temperature. It is therefore evident that any cleaning of Ge/GeSn surfaces has strong constrains in terms of maximum process temperature.

In this work, we present a new method to clean Ge/GeSn surfaces: by using a hot-wire activated hydrogen atmosphere, we have cleaned $Ge/Ge_{0.9}Sn_{0.1}$ heterostructures deposited *ex situ* by reduced-pressure chemical vapor deposition (RP-CVD) at very low temperature (∼100 °C).

This epi-cleaning technique, which has been first proposed in the nineties to achieve clean and reconstructed surfaces in III–V materials,[13,14] is based on the surface atom etching by atomic hydrogen. The atomic hydrogen is obtained by high purity H_2 molecule cracking from a

a)Author to whom correspondence should be addressed. Electronic mail: capellini@ihp-microelectronics.com

metallic hot wire placed in the vicinity of the sample surface. The etching occurs because the impinging H atoms break surface atom bonding and induce the formation of H-radicals by subsequent H inclusion, which eventually are bounded loosely enough to be desorbed, in the present case as GeH_x, H_2O, and CH_x molecules.[15]

The analysis performed by x-ray photoemission spectroscopy (XPS), reflection high-energy electron diffraction (RHEED), atomic force microscopy (AFM), x-ray diffraction and reflectivity measurements (XRD/XRR), secondary ion mass spectroscopy (SIMS), and micro-Raman analysis has evidenced that the proposed technique leads to epi-ready quality, contamination-free, reconstructed surface in which the initial strain and morphology are not affected by the cleaning process. This method could also be applied to Ge/Si heterostructures or germanium on insulator and Ge substrates, preventing intermixing and agglomeration phenomena.

EXPERIMENTAL

The tensile strained Ge/GeSn heterostructure growth was performed in an industry-compatible 200 mm wafer RP-CVD AIXTRON TRICENT® reactor using Ge_2H_6 and $SnCl_4$ precursors. High quality (Si)GeSn epitaxy has been presented in previous investigations.[6] The lattice parameter of GeSn strain-relaxed buffers (SRBs) is given by the degree of strain relaxation and the Sn content, which can be precisely tuned by varying the growth temperature. In order to increase the in-plane lattice constant of SRBs, 200–300 nm thick layers have been grown, that is exceeding the critical thickness for strain relaxation. The strain relaxation of (Si)GeSn layers is mediated by the nucleation and propagation of misfit dislocations. In all transmission electron microscopy (TEM)-analyzed GeSn alloys grown on high quality Ge(001) virtual substrates (Ge-VS), threading dislocations density was below the detection limit ($<10^6\,cm^{-2}$). In Fig. 1(a), we present the TEM micrograph of the sample used in this study, featuring a 65 nm thick tensile strained Ge layer deposited on a 300 nm-thick GeSn layer grown on top of a relaxed Ge/Si(001) virtual substrate. While we can see defects at the GeSn/Ge-VS interface and dislocation loops in the Ge virtual substrate, the s-Ge/GeSn interface appears defect-free.

The analysis of reciprocal space map (RSM) around the Ge $(\bar{2}\bar{2}4)$ point performed by high resolution XRD (see Fig. 1(b)) evidences that the Ge layer has a $\varepsilon_{par} \sim 1\%$ in plane tensile strain, while the $Ge_{1-x}Sn_x$ layer has a tin content $x = 0.1$ and its level of relaxation is 99%.

The substrates were cut into $2 \times 1\,cm^2$ pieces, packaged in clean-room conditions in FZ-Juelich, and sent to Roma Tre University, where the clean-box has been opened in a clean environment under a laminar flow hood. Then, the samples were cleaned with an isopropyl alcohol bath followed by N_2 blowing, mounted on the sample holder, and immediately loaded in the UHV system through a fast entry load lock. All the investigated samples were cut from the same 200 mm wafer.

The cleaning experiment was carried out in an ultra-high vacuum CVD reactor, whose base pressure is $\sim 2 \times 10^{-10}$ Torr. The atomic hydrogen was generated by contact catalysis on a tungsten hot-wire catalyzer placed ~10 cm from the sample surface. The W-filament was set at a temperature of T = 1600 °C by Joule heating. The standard cleaning process time was chosen to be 10 min. The sample temperature was controlled by directly flowing a DC electrical current and measured by an infrared pyrometer with an accuracy of ±5 °C for temperature values down to 250 °C. For lower values, the sample T was extrapolated by measuring the sample resistance using a calibration table obtained by means of a contact thermocouple on a selected sample with the W filament being both on and off. We estimated a ±20 °C measurement accuracy in this case.

After the cleaning process, the samples were transferred under UHV conditions to an analytical chamber equipped with a XPS system and a 10 keV RHEED system. *In situ* XPS measurements were performed using a monochromatic Al K_α source ($h\nu = 1486.6$ eV) and a concentric hemispherical analyzer operating in retarding mode (Physical Electronics Instruments PHI); the overall spectral resolution was 0.35 eV.

The sample morphology was investigated *ex situ* by means of a Veeco CP-II AFM, operating in contact mode using high aspect ratio tips with a nominal tip radius of 5 nm. The surface roughness and the structural properties were investigated by XRR and XRD measurements. All x-ray measurements were carried out with a SmartLab diffractometer from Rigaku equipped with a 9 kW rotating anode Cu source in line focus geometry. The standard diffractometer scheme for high resolution specular XRD and XRR measurements consists of an x-ray mirror in combination with a two-fold Ge (400) crystal collimator. For RSM, a Ge(220 × 2) analyzer crystal was used additionally.

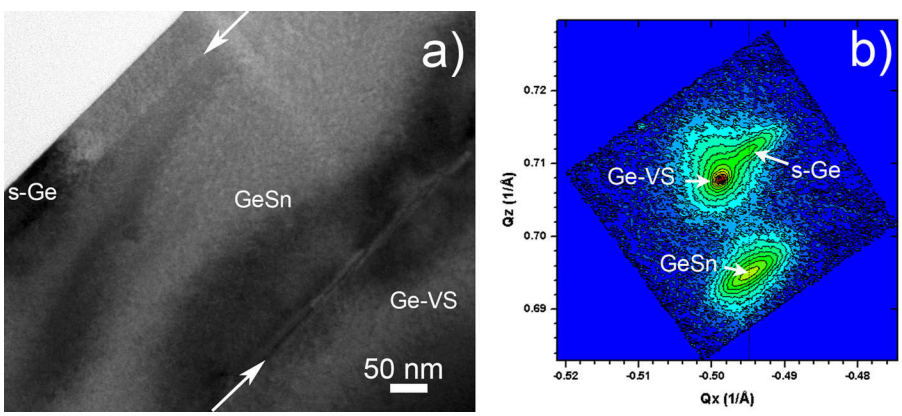

FIG. 1. (a) Cross section TEM of the as-received sample and (b) XRD-RSM acquired around the $(\bar{2}\bar{2}4)$ reciprocal lattice point. The different contributions of the three layers are indicated.

The strain analysis was also complemented by Raman spectroscopy. Raman measurements were performed by using a Labram Micro-Raman spectrometer by Horiba, equipped with a He-Ne laser sources at 632.8 nm (nominal output power 18 mW). The illumination and collecting optics of the system consists in a microscope in confocal configuration. Nominal spectral resolution was $\sim 1\,cm^{-1}$. The investigation of Sn diffusion was performed by SIMS using a Cs^+ primary beam.

RESULTS

In Fig. 2, we display the XPS spectra of two samples sets as a function of the electron binding energy E_b. The data acquired on samples annealed at different temperature in H_2 atmosphere ($P = 0.5$ mTorr) without (left column) or with (right column) hydrogen activation by hot wire are presented. Data for as-received samples (continuous lines), and for samples processed at 100 °C (blue squares) and 300 °C (red circles) are presented. From top to bottom panels, we report the spectral regions relative to the Ge_{3d}, $Ge_{2p3/2}$, C_{1s}, O_{1s}, and Sn_{3d} core levels, respectively. All the spectra have been normalized to the integrated intensity of the Ge_{3d} core levels (Figs. 2(a) and 2(a′)).

The as-received samples XPS spectra feature a clear signature arising from carbon and oxygen surface contamination due to its exposure to the water and the hydrocarbons present in the laboratory atmosphere, with a relatively high photoemission signals from the C_{1s} ($E_b \sim 284$ eV, Figs. 2(c) and 2(c′)) and O_{1s} ($E_b \sim 533$ eV panels (d) and (d′)).

The C_{1s} lineshape results from the contribution of a main peak at lower binding energy (284.5 eV) attributed to hydrocarbon-Ge-C bonds, the so-called adventitious carbon, and to a higher energy shoulder due to C-O bonding.[16] As expected, since the thickness of the strained Ge layer is well above the typical electron escape depth (0.5–5 nm) no contribution from the Sn atoms in the GeSn layer was detected (panels (e) and (e′)).

In the Ge_{3d} and $Ge_{2p3/2}$ spectra, the two components corresponding to the emission from the elemental Ge and from its oxide, chemically shifted at higher binding energy, are well visible. Due to the higher surface sensitivity of the Ge_{2p} photoelectrons in the 2p spectra, the Ge-oxide component has higher intensity than the Ge-Ge one. The chemical shifts of the oxide-related components, equal to about 3.4 eV for both the Ge_{3d} and $Ge_{2p3/2}$ core levels, indicate that the oxide layer is mainly stoichiometric GeO_2, in agreement with the formation of the Ge oxide layer by relatively long air exposition of the samples after the growth and with the measured O_{1s} peak position.[17] XPS measurements shown in the left panels show that the sample heating at 100 °C or 300 °C in a molecular H_2 atmosphere for 10 min is practically ineffective in removing the oxide (only a 10% reduction of the ratio between O and Ge emission intensities is found). On the contrary, this process step reduces the adventitious C contamination. After the 300 °C annealing, the C contamination is 1/3 of its initial value, thanks to the partial desorption of the hydrocarbon volatile species physisorbed on the Ge oxide surface and to the desorption of the C-O compounds, the latter evidenced by the disappearance of the higher binding energy component of the C_{1s} lineshape ($E_b \sim 286.5$ eV for C-O bonding[16]). Nevertheless, a significant residual C contamination (~8%) is still present on the sample surface and this residual value is not reduced by increasing the annealing time to 50 min (not shown). Finally, as shown in panel (e), no emission from Sn_{3d} core level is detected after the two annealing procedures, indicating that no Sn segregation

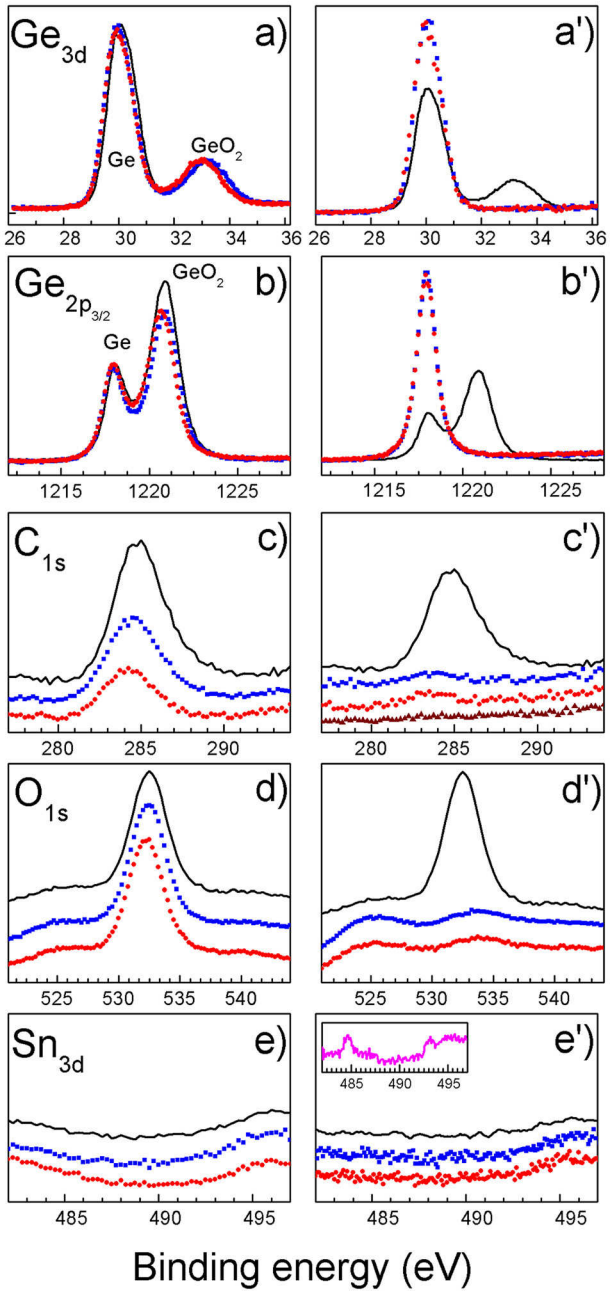

FIG. 2. XPS spectra of Ge_{3d}, Ge_{2p}, C_{1s}, O_{1s}, and Sn_{3d} core levels taken on samples after heating in molecular H_2 atmosphere (left panels) and in activated hydrogen atmosphere (right panels) for a process time of 10 min. Continuous black lines refer to the as-received samples, blue squares and red circles to samples cleaned at 100 °C and 300 °C, respectively. Spectra acquired in the as-received samples are reported in both left and right panels for comparison. Triangles in panel c′ refer to C_{1s} spectrum acquired after an annealing at 100 °C in atomic hydrogen for 45 min. Inset of panel e′: the $Sn3_d$ spectrum acquired after the sample heating at 400 °C in atomic hydrogen for 5 min. Spectra are vertically shifted for clarity.

towards the surface was promoted by heating up to 300 °C, i.e., above the GeSn eutectic temperature.

This scenario drastically changes if the hydrogen molecules are activated by the hot tungsten filament, as can be observed in the right panels of Fig. 2. At a process temperature as low as 100 °C (right panels), we observe the removal of the oxide layer from the sample surface, as demonstrated by the disappearance of the contribution from both Ge-O related feature and O_{1s} core level in the XPS spectra shown in panels (a′), (b′), and (d′). We point out that the spectral features observed at 525 eV and 534 eV are due to the Ge $L_2M_{23}M_{23}$ Auger peaks and are thus not related to O. In this process conditions, we also found a strong decrease of the C-related photoemitted intensity, with the emission from C_{1s} level approaching the instrumental sensitivity (Fig. 2(c′)). A carbon free Ge surface, i.e., a surface featuring a C contamination below the detectability limit of the XPS technique (0.1%), is achieved protracting the heating at 100 °C for 50 min (panel (c′), triangles). The results obtained upon processing the samples in activated atomic hydrogen at higher temperature (T = 300 °C) are nearly identical to those discussed from the point of view of the surface cleanliness.

The crucial role of the temperature for the stability of the Ge/GeSn structures is highlighted by the XPS measurements acquired on a sample annealed at 400 °C for 5 min in activated hydrogen, reported in the inset of Fig. 2. The emission from Sn $3d_{5/2,3/2}$ are well visible in the spectrum confirming that this process temperature induces strong Sn segregation on the surface. As also confirmed by SIMS analysis (Fig. 3(a)), at lower process temperature the diffusion of Sn atoms from the VS to the Ge epi-layer is negligible: the leading edge slope of the Sn^{120} signal is ∼4 nm/decade for both samples.

The cleaning process does not impact the surface morphology nor the strain status of the samples as can be observed in Fig. 3(b), where we present two AFM images of the as-received sample (bottom-left) and of the 300 °C-annealed sample (top-right) together with their corresponding XRR spectra. The surface morphology shows the characteristic [110]-aligned cross hatch pattern due to the plastic relaxation of the underlying virtual substrate[6] with nearly identical roughness (RMS roughness ∼1 nm in an analyzed area of 100 μm^2).

Moreover, the top Ge layer thickness is only slightly affected by the activated H removal of the surface contamination as determined by XRR analysis. For both samples, even if the difference in electron density between the GeSn and Ge epi-layer is relatively low, oscillations could be observed in the XRR measurements. These oscillations are due to the interference of the reflected x-rays at the epi-layer interfaces and are used to calculate the thickness of the Ge epi-layer by means of the simulation software RCRefSimW.[18] We can evaluate, with an accuracy better than 1 nm, a thickness t_{Ge} = 64.2 nm for the as-received sample and t_{Ge} = 62.3 nm for the 300 °C-annealed sample, respectively. This moderate reduction of the thickness could also be compatible with thickness variation over the wafer occurring during the sample growth. The roughness of the two samples calculated from the XRR data was 1.2 nm in both cases, in good agreement with the AFM determination.

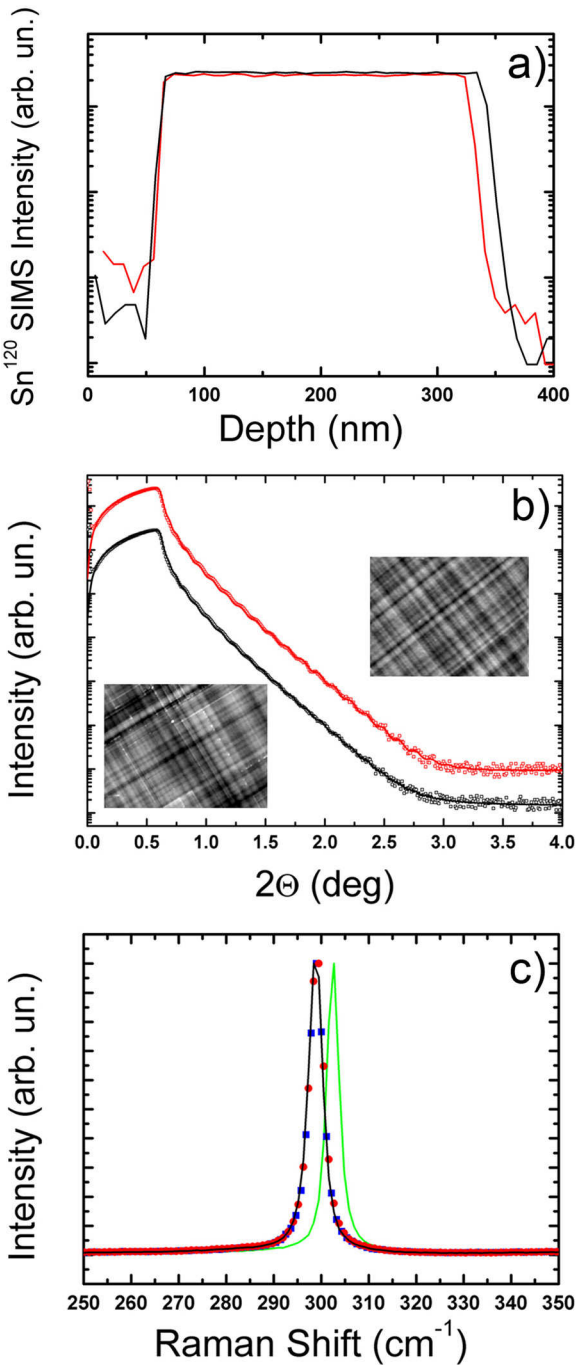

FIG. 3. (a) SIMS profile for the Sn120 ion measured for the as-received (black) and 300 °C annealed (red) samples; (b) 10 × 7.5 μm^2 AFM images of the as received sample (bottom-left) and 300 °C annealed (top-right). The cross-hatch lines are aligned along [110]-equivalent directions. In the same panel, we also report the XRR spectra for the two samples: black line is for the as-received and red for the annealed. Spectra have been shifted for improved visibility. (c) Raman spectra for a Ge reference wafer (green), as-received Ge/GeSn substrate (black), sample cleaned at 100 °C (blue), and at 300 °C (red).

The moderate thermal budget of the proposed cleaning method does not induce any strain relaxation of the Ge epi-layer, as can be observed in Fig. 3(c), where we show the Raman spectra of a Ge bulk reference (green), of the as-received Ge/GeSn sample (black), and of both the 100 °C

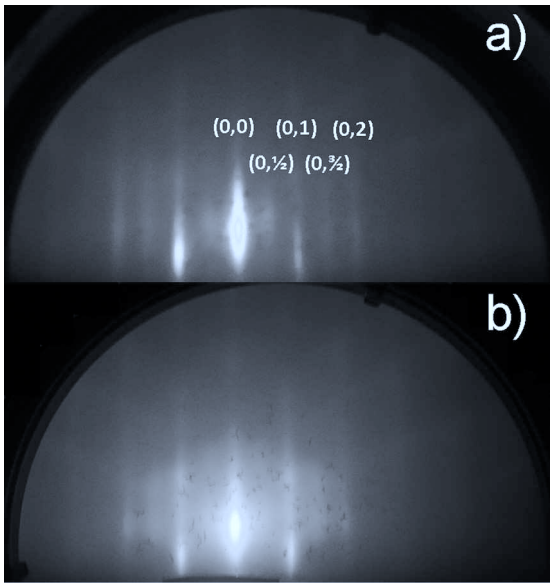

FIG. 4. RHEED patterns of Ge/GeSn samples cleaned in atomic hydrogen at (a) 300 °C and (b) 100 °C, respectively.

and 300 °C annealed samples. The penetration depth of the 633 nm laser used is limited to 32 nm, i.e., ∼half the Ge epi-layer thickness, and thus the signal from the plastically relaxed substrate or of Ge-Ge modes in the GeSn layer is highly reduced. The three curves corresponding to Ge/GeSn samples are undistinguishable and they reflect, following the method in Ref. 19, an in plane strain in the Ge epi-layer of 1.1%, a value in very good agreement with that obtained by XRD (see Fig. 1).

Finally, we show that the cleaning procedure leads to a good surface crystal quality of the Ge epi-layer, ready for a subsequent epitaxial growth of high quality. Figs. 4(a) and 4(b) report the RHEED patterns of the Ge/GeSn samples after the cleaning procedure at 300 °C and 100 °C, respectively. The azimuthal direction was the [110]. In both samples, we observed a streaky pattern compatible with a flat, 2×1 reconstructed Ge surface. The main difference between the two samples is the higher diffuse scattering visible in the 100 °C sample. This "halo" evidences a pre-amorphization of the surface. We attribute it to the very low process temperature, which hinders the surface diffusion and "self-healing" after the H ion-induced removal of the topmost surface layer. We thus believe that this temperature represents a lower limit for the achievement of an epi-ready surface using the proposed cleaning process.

CONCLUSIONS

In summary, we have demonstrated an *in situ* method suitable for surface cleaning of Ge/GeSn(001) heterostructures based on exposure to activated hydrogen ions. We have achieved C- and O-free surface while preserving epi-ready surface quality at process temperature as low as 100 °C. A thorough structural investigation ruled out any unwanted strain relaxation or Sn segregation during the process. This method is also straightforwardly applicable to any Ge surface, including Germanium-on-insulator layer, Ge/Si heterostructures, and Ge bulk samples.

[1]E. Kasper, M. Kittler, M. Oehme, and T. Arguirov, Photonics Res. **1**, 69 (2013).
[2]J. Menéndez and J. Kouvetakis, Appl. Phys. Lett. **85**, 1175 (2004).
[3]S. Chang and S. L. Chuang, J. Quantum Electron. **43**, 249 (2007).
[4]G. Sun, R. A. Soref, and H. H. Cheng, J. Appl. Phys. **108**, 033107 (2010).
[5]M. Virgilio, C. L. Manganelli, G. Grosso, G. Pizzi, and G. Capellini, Phys. Rev. B **87**, 235313 (2013).
[6]S. Wirths, D. Buca, Z. Ikonic, P. Harrison, A. T. Tiedemann, B. Holländer, T. Stoica, G. Mussler, U. Breuer, J. M. Hartmann, D. Grützmacher, and S. Mantl, Thin Solid Films **557**, 183 (2014).
[7]S. Wirths, A. T. Tiedemann, Z. Ikonic, P. Harrison, B. Holländer, T. Stoica, G. Mussler, M. Myronov, J. M. Hartmann, D. Grützmacher, D. Buca, and S. Mantl, Appl. Phys. Lett. **102**, 192103 (2013).
[8]C. Blumenstein, S. Meyer, A. Ruff, B. Schmid, J. Schäfer, and R. Claessen, J. Chem. Phys. **135**, 064201 (2011).
[9]L. Chu, Y. C. Liu, W. C. Lee, T. D. Lin, M. L. Huang, T. W. Pi, J. Kwo, and M. Hong, Appl. Phys. Lett. **104**, 202102 (2014).
[10]M. Klesse, G. Scappucci, G. Capellini, and M. Y. Simmons, Nanotechnology **22**, 145604 (2011).
[11]L. H. Chan, E. I. Altman, and Y. Liang, J. Vac. Sci. Technol., A **19**, 976 (2001).
[12]P. Ponath, A. B. Posadas, R. C. Hatch, and A. A. Demkov, J. Vac. Sci. Technol., B **31**, 031201 (2013).
[13]T. Sugaya and M. Kawabe, Jpn. J. Appl. Phys., Part 2 **30**, L402 (1991).
[14]Y. J. Chun, T. Sugaya, Y. Okada, and M. Kawabe, Jpn. J. Appl. Phys., Part 2 **32**, L287 (1993).
[15]A. Izumi, H. Sato, S. Hashioka, M. Kudo, and H. Matsumura, Microelectron. Eng. **51–52**, 495 (2000).
[16]T. L. Barr and S. Seal, J. Vac. Sci. Technol., A **13**, 1239 (1995).
[17]P. Prabhakaran and T. Ogino, Surf. Sci. **325**, 263 (1995).
[18]See http://www.ihp-ffo.de/en/services/xrr-hrxrd-simulation/overview.html for XRR/XRD simulation software RCRefSimW.
[19]G. Capellini, M. De Seta, Y. Busby, M. Pea, F. Evangelisti, G. Nicotra, C. Spinella, M. Nardone, and C. Ferrari, J. Appl. Phys. **107**, 063504 (2010).